Virology Journal

RESEARCH

Open Access

Comparative evaluation of immunomodulatory cytokines for oncolytic therapy based on a high-efficient platform for oHSV1 reconstruction

Yingzheng Gao[1,2†], Yufang Zou[1,2†], Changjing Wu[1,2†], Juan Tao[1,2], Zuqing Nie[1,2], Jinyuan Yan[1,2], Pengfei Wang[1,2*] and Xinwei Huang[1,2*]

Abstract

Background Triple-negative breast cancer (TNBC) presents significant therapeutic challenges due to its immunosuppressive tumor microenvironment (TME). Oncolytic herpes simplex virus type 1 (oHSV1) offers dual mechanisms of tumor lysis and immune activation, yet the optimal cytokine payloads for TNBC remain undefined.

Methods We developed a CRISPR/Cas9-mediated platform for high-efficiency oHSV1 engineering, replacing the ICP47 locus with murine IFN-γ, GM-CSF, or IL-15Rα/IL-15 fusion protein (IL15Fu). Constructs were validated for cytokine secretion, MHC modulation, and cytotoxicity in 4T1 TNBC and a panel of human cancer cell lines. Antitumor efficacy and immune remodeling were evaluated in a syngeneic 4T1 model using RNA sequencing and flow cytometry.

Results The CRISPR platform achieved 62.5–71.4% homologous recombination efficiency, enabling rapid virus construction. In vitro, OV-IFNG exhibited upregulated MHC I/II expression and potent cytotoxicity, while OV-GMCSF attenuated oncolysis in subsets of breast cancer cell lines. In the 4T1 model, OV-IL15Fu modestly improved tumor control and extended survival without apparent toxicity, while OV-IFNG induced early mortality associated with systemic toxicity. Transcriptomic profiling revealed divergent immune modulation: OV-IL15Fu enriched T cell/NK cytotoxicity pathways, OV-IFNG amplified cytokine/chemokine signaling, and OV-GMCSF paradoxically enhanced myeloid recruitment while inhibiting MHC-II pathways. Flow cytometry confirmed functional differences in immune activation: OV-IL15Fu expanding cytotoxic lymphocytes ($CD8^+$ T/NK cells), OV-IFNG preferentially promote Th1 polarization and innate immune activation, and OV-GMCSF failed to activate T cells despite myeloid infiltration.

Conclusions Our findings underscore the need for rational cytokine selection in oHSV1-based immunotherapy. While IFN-γ increased immunogenic markers, its systemic toxicity and myeloid effects may limit benefit. GM-CSF

†Yingzheng Gao, Yufang Zou and Changjing Wu contributed equally to this work.

*Correspondence:
Pengfei Wang
wangpengfei@kmmu.edu.cn
Xinwei Huang
huangxinwei@kmmu.edu.cn

Full list of author information is available at the end of the article

exacerbated immune suppression in this context, whereas IL15Fu showed favorable immunostimulatory properties without detectable toxicity. These data support IL15Fu as a contextually promising payload for further evaluation in TNBC-targeted oncolytic virotherapy.

Keywords Oncolytic virus, HSV-1, Immunomodulatory cytokines, GM-CSF, IFN-γ, IL15Rα/IL15 fusion protein

Introduction

TNBC, characterized by the absence of estrogen receptor, progesterone receptor, and HER2 amplification, remains a formidable clinical challenge due to its aggressive biology, metastatic propensity, and resistance to targeted therapies [1]. The immunosuppressive TME of TNBC—dominated by myeloid-derived suppressor cells (MDSCs), dysfunctional dendritic cells (DCs), and scarce tumor-infiltrating lymphocytes (TILs)—further undermines the efficacy of conventional immunotherapies such as immune checkpoint inhibitors [2]. oHSV1 has emerged as a promising multimodal therapy, combining direct tumor lysis with immunogenic cell deathmediated immune activation [3]. Genetic arming of oHSV1 with immunomodulatory cytokines is a rational strategy to boost these effects. However, most prior studies have evaluated single cytokines in isolation, with limited attention to tumor-specific immune context or comparative mechanistic analysis [4].

Cytokine selection for oHSV1-based therapy must account for more than immune stimulation; it requires careful balancing of efficacy, safety, and tumor-context specificity. While cytokines such as IL-12 and IFN-γ have potent immunostimulatory potential, their overlapping mechanisms and systemic toxicity complicate their translational utility. For instance, IL-12 acts largely through downstream IFN-γ induction [5, 6], making it less suitable for side-by-side comparison with IFN-γ itself in efforts to deconvolute cytokine-specific effects. To avoid redundancy and maximize mechanistic contrast, we selected three cytokines—IFN-γ, granulocyte-macrophage colony-stimulating factor (GM-CSF), and IL15Fu—based on their distinct immunological roles in modulating the TME: (1) IFN-γ directly enhances tumor immunogenicity by upregulating MHC class I/II and antigen-processing machinery (e.g., TAP1/2) via JAK/STAT1 signaling [7], addressing antigen presentation deficiencies in TNBC. (2) GM-CSF, the cytokine payload in FDA-approved T-VEC for melanoma [8], promotes DC recruitment and maturation, but in breast cancer models, it has also been implicated in MDSC expansion and tumor progression [9]. (3) IL15Fu, a fusion of IL-15 and IL-15Rα, supports the proliferation and survival of NK cells and memory phenotype $CD8^+$ T cells via trans-presentation, without triggering regulatory T cell activation—making it particularly appealing in lymphocyte-depleted TMEs [10]. Importantly, IFN-γ was included in this study not as a therapeutic recommendation, but as a mechanistic comparator to explore the immunologic consequences of potent Th1 polarization and MHC upregulation in a highly suppressive TNBC model. Its inclusion allows us to delineate the trade-offs between immune activation and systemic toxicity, consistent with prior reports of its dual effects in cancer biology [11].

To facilitate systematic evaluation, we developed a CRISPR/Cas9-based engineering platform enabling high-efficiency homologous recombination at the ICP47 locus, achieving 62.5–71.4% insertion efficiency—streamlining the generation of cytokine-armed oHSV1 variants [12, 13]. This platform allowed us to compare, within a uniform viral backbone, how IFN-γ, GM-CSF, and IL15Fu differentially influence antigen presentation, immune cell composition, and therapeutic response in vitro and in vivo in the immune-resistant 4T1 TNBC model. This study aimed to address the following key questions: (1) How do these cytokines differentially reprogram the TNBC immune microenvironment when delivered by oHSV1? (2) Can cytokine engineering overcome known limitations of virotherapy in immunosuppressive tumor settings? (3) What are the immune-functional and safety trade-offs among commonly used cytokine payloads?

Rather than proposing a new cytokine for clinical use, this work provides a comparative framework for rational cytokine selection in oHSV1 therapy—one that prioritizes context-specific immune barriers over empirical use of broadly "proinflammatory" cytokines. Our findings underscore that cytokine efficacy and safety are highly dependent on tumor context, and highlight IL15Fu as a promising candidate for further investigation in TNBC-targeted oncolytic immunotherapy.

Methods

Animal and cell lines

The animal experiments were conducted in accordance with the guidelines and regulations of Animal Experiment Ethics Review Committee of Kunming Medical University. Six-week-old female BALB/c mice were obtained from Charles River Laboratories in Beijing and housed in specific pathogen free facilities.

The cell lines utilized in this research were obtained from the National Biomedical Experimental Cell Resource Bank in Kunming, China. Specifically, 293T cells were employed for plasmid transfection and virus construction. Vero cells were utilized for viral propagation and plaque-assay-based viral titration. The human breast cancer cell lines (MDA-MB-231, MCF-7,

HCC1937), human malignant melanoma cell lines (A375, A2058), human colon cancer cell lines (HCT-116, SW620) and human hepatocellular carcinoma cell lines (HepG2) were utilized for CCK8 assay and analysis of gene expression. B16F10-mTNFRSF14 cells were generated through lentivirus infection and puromycin selection. Additionally, 4T1 cells were used to establish a syngeneic mouse model of triple negative breast cancer. HCC1937 cells were cultured in RPMI 1640, other cell lines were cultured in DMEM supplemented with 10% FBS, penicillin (100 U/mL), and streptomycin (100 μg/mL) at 37℃ and 5% CO2.

Oncolytic virus construction based on CRISPR-Cas9 gene editing

The attenuated HSV-1 Strain (1716 Strain) utilized in this research was graciously provided by Professor Nigel William Fraser from the University of Pennsylvania. The CRISPR-Cas9 plasmid (Px458, plasmid # 48138) was procured from Addgene. Guide RNA sequences targeting the US12 locus and mCherry reporter gene were designed using Benchling online (http://www.benchling.com) to minimize mismatches (US12-1.1: ATT-GATCTC ATCGCGTACGT, mCherry1.1: GGCCACGAGTTCGA GATCGA, mCherry1.2: GAACAGTACGAACGCGCCG A). Forward and reverse strands were synthesized based on the cohesive end of BbsI restriction enzyme sites in the Px458 vector. Primers located adjacent to the target site on the US12 locus (TestxF: GATCGCATCGGAAA GGGACA; TestxR: CGCACCGACTCGTAGTAGAC) were utilized for the purpose of detecting gene deletions or insertions.

A two-step strategy was is used to construct oncolytic virus armed with therapeutic genes on the background of HSV-1 1716 strain. First, the viral gene US12 (encoding ICP47) was replaced with mCherry reporter gene. 293T cells were co-transfected with donor plasmid containing homology arms of ICP47 flanking a mCherry-P2A coding sequence and the CRISPR-Cas9 expression plasmid US12-1.1. After transfection and cell recovery, 293T cells were infected with HSV-1 1716 at multiplicity of infection (MOI) = 1. The resulting virus was inoculated to Vero cells overlaid with DMEM medium containing 2% methyl-cellulose, and the mCherrypositive recombinant (named OV-mCherry) were identified under inverted fluorescent microscope. Second, the mCherry reporter gene was replaced with murine therapeutic genes (GM-CSF, IFN-γ, IL15Fu). 293T cells were co-transfected with donor plasmids containing homology arms of ICP47 flanking a GM-CSF/IFN-γ/IL15Fu-P2A coding sequence and a pair of CRISPR-Cas9 expression plasmid mCherry1.1 and mCherry1.2 which target the both ends of mCherry gene. Then the cells were infected with parental virus OV-mCherry at MOI = 1. The recombinant virus, in which the mCherry gene was replaced with a therapeutic gene, was isolated on Vero cells overlaid with DMEM medium containing 2% methylcellulose. This isolation was based on the absence of mCherry fluorescence and was subsequently confirmed through PCR-sequencing using primers that flank the ICP47 locus (TestxF/TestxR).

Oncolytic virus Preparation and Titration

The oncolytic viruses were propagated on Vero cells then purified by sucrose density gradient centrifugation. Briefly, the indicated virus infected Vero cells (80%~85% cell confluency) at MOI = 0.5. After 4 days' incubation, the supernatant was collected and centrifuged at 4000*rpm* for 10 min to remove the residual cellular debris. Collected supernatant wasfurther filtered through a 0.45 μm PVDF Millipore membrane filters then overlayed on 20% (W/V) sucrose solution and centrifuged at 26000*rpm* for 3 h. Purified viruses were re-suspended in PBS solution and stored at -80℃.

The viral titer was determined by counting the number of plaques on Vero monolayer cells (a culture medium containing 1.5% methylcellulose for 4 days) infected with serial dilutions of the virus.

Enzyme-linked immunosorbent assay

4T1 tumor cells were infected with indicated viruses at MOI = 1. After 24 or 48 h, supernatants of the tumor cell cultures were collected. GM-CSF and IFN-γ secreted by infected cells were determined using Mouse GM-CSF ELISA Kit (Proteintech, Cat No. KE10015) and Mouse IFN-gamma ELISA Kit (Proteintech, Cat No. KE10094) respectively, according to the manufacturer's instructions. The secretion of the IL15Rα/IL15 fusion protein into the culture supernatants from OV-IL15Fu infected cells was quantified using the Mouse IL-15/IL-15R Complex Mouse ELISA Kit (Invitrogen, BMS6023) following the manufacturer's guide.

Flow cytometry assay of tumor cell MHC expression

A Flow cytometry assay was used to determine the cell surface expression of MHCI and MHCII on 4T1 cells infected with oncolytic virus. Tumor cells were inoculated with indicated oHSV1s at MOI = 1 for 24 h. Then the cells were harvested and fixed with Fixation Buffer (BioLegend, 420801). After washing with Cell Staining Buffer (BioLegend, 420201), cells were stained with APC anti-mouse H-2Kd/H-2Dd (BioLegend, 114714) and PE anti-mouse I-A/I-E Antibody (BioLegend,107607). Cells strained with isotype antibody with same fluorescein were used as background control. The expression level was indicated by mean fluorescence intensity (MFI).

In vitro assay of cytotoxic effects of cytokine armed oncolytic virus

Cell lines were inoculated into 96-well plates (1×10^4 cells/well) overnight and then infected with various oHSV1s at indicated MOIs. Cell viability was measured by the cell counting kit-8 (CCK8, Biosharp, BS350B) following the manufacturer's instructions. At the indicated time points, the cells were incubated with CCK8 solution for 2 h at 37 °C and were determined with a microplate spectrophotometer (Thermo, Multiskan Sky, 51119670) by absorbance at 450 nm. The relative cell viability ratio of tumor cells was calculated as follows: (OD value of infected cells-OD value of Black) / (OD value of uninfected cells-OD value of Black) × 100% to evaluate the in vitro cytotoxic effect of various oHSV1s.

Murine tumor models and treatments

For murine syngeneic tumor models, 2×10^5 tumor cells in 75μL of PBS-Matrigel (Corn-ing,354263) mixture (1:1) were subcutaneously inoculated into the right flank of 6week-old BALB/c mice by disposable insulin syringe (BD). When the tumor size reached around 100 mm^3(designated as Day 1), the mice were randomly divided into groups (8 mice per group) followed by intratumoral injection of 1×10^7 PFU armed oHSV1s four times on days 1, 3, 5 and 7, control mice were treated same volume of PBS. The tumor growth was monitored by caliper every three days according to the formula: $0.5 \times Length \times (Width)^2$. When the tumor volume reached 2000 mm^3, mice were euthanized and recorded the time of death.

RNA sequencing and data analysis

The tumor tissue for RNA sequencing analysis was obtained through surgical resection of mice from different treatment groups. Gene expression data (FPKM and read counts) that met quality control requirements were collected, followed by statistical analysis to identify significant differential genes (DEGs). In this process, upregulated or downregulated genes were defined as those with significantly increased or decreased expression compared to the reference group. Differential gene selection criteria included a P value < 0.05 and |Log2FoldChange| > 0.5. Subsequently, the Cluster Profiler package was employed to perform enrichment analyses using Gene Ontology (GO, http://www.geneontology.org/) and Kyoto Encyclo pedia of Genes and Genomes (KEGG, https://www.kegg.jp/), aiming to explore potential functions associated with these significant differential genes and obtain gene lists enriched in specific functions or pathways along with their respective quantity statistics. Finally, visualization of the enrichment analysis results was achieved using the ggplot2 package and Complex-Heatmap package.

Flow cytometry analysis of tumor-infiltrating immune cells and spleen cells

In the 4T1 Syngeneic tumor model, mice were intratumoral injection with 1×10^7 PFU or same volume of PBS on day 1. One week post treatment, tumor tissue was collected and minced into 1 ~ 2 mm small pieces and washed with PBS containing 2% penicillin/streptomycin, then digested with Liberase DL (Roche, 2.5 mg/ml, 200 μl,), Liberase TL (Roche, 2.5 mg/ml, 200 μl,), hyaluronidase (Solarbio, 15 mg/ml, 100 μl) and DNase I (Solarbio, 15 mg/ml, 100 μl) incubated for 1 h 30 min with horizontal shaking at 120 rpm, 37 °C. The tumor tissues were homogenized and then filtered through a 70 μm cell nylon strainer. Single-cell suspensions were counted and collected. In addition, PBMC suspension was prepared by spleen were isolated from various oHSV1-treated tumor-bearing BALB/c mice and centrifugation according to the method described in the instructions (DKW33-R0100, DAKEWE). The single cells were stained with Zombie Aqua viability dye (BioLegend), followed by Fc receptor blockade (CD16/32, BioLegend, clone 93). For intracellular cytokine staining, the cells were fixed and permeabilized with eBioscience Intracellular Fixation & Permeabilization Buffer set, then stained with BioLegend lymphocyte panel antibodies: CD4-FITC (RM4-5), CD8-PerCP/Cy5.5 (53 – 6.7), CD49b-APC (DX5), GZMB-BV421 (QA16A02) and IFN-γ-PE/Cy7 (XMG1.2). For cell surface marker staining, the single cells were Fixed with BioLegend Fixation Buffer, then stained with BioLegend myeloid panel antibodies: CD45-FITC (30-F11), CD11b-PerCP/Cy5.5 (M1/70), CD11c-BV605 (N418), Ly6G-APC (1A8), Ly6C-APC/Cy7 (HK1.4), F4/80-BV421 (BM8), MHCII-PE (I-A/I-E, M5/114.15.2). Samples were acquired on a Beckman DxFLEX cytometer and analyzed in FlowJo V10 software using strategies according to previous studies [14].

Statistical analysis

The experimental data analysis was conducted using GraphPad Prism software. One-way ANOVA was utilized to analyze ELISA measures, flow cytometry assay, and CCK8 assay results. The growth curves of 4T1 tumors were analyzed using two-way ANOVA with multiple comparisons. Animal survival was assessed using the Kaplan-Meier survival curves method and statistical significance was determined using the two-tailed log rank (Mantel-Cox) test.

Results

Construction of oncolytic HSV-1 armed with Immunomodulatory cytokines by CRISPR-Cas9 mediated gene editing

As reported, the HSV-1 viral gene product ICP47 could target the cellular transporter associated with antigen

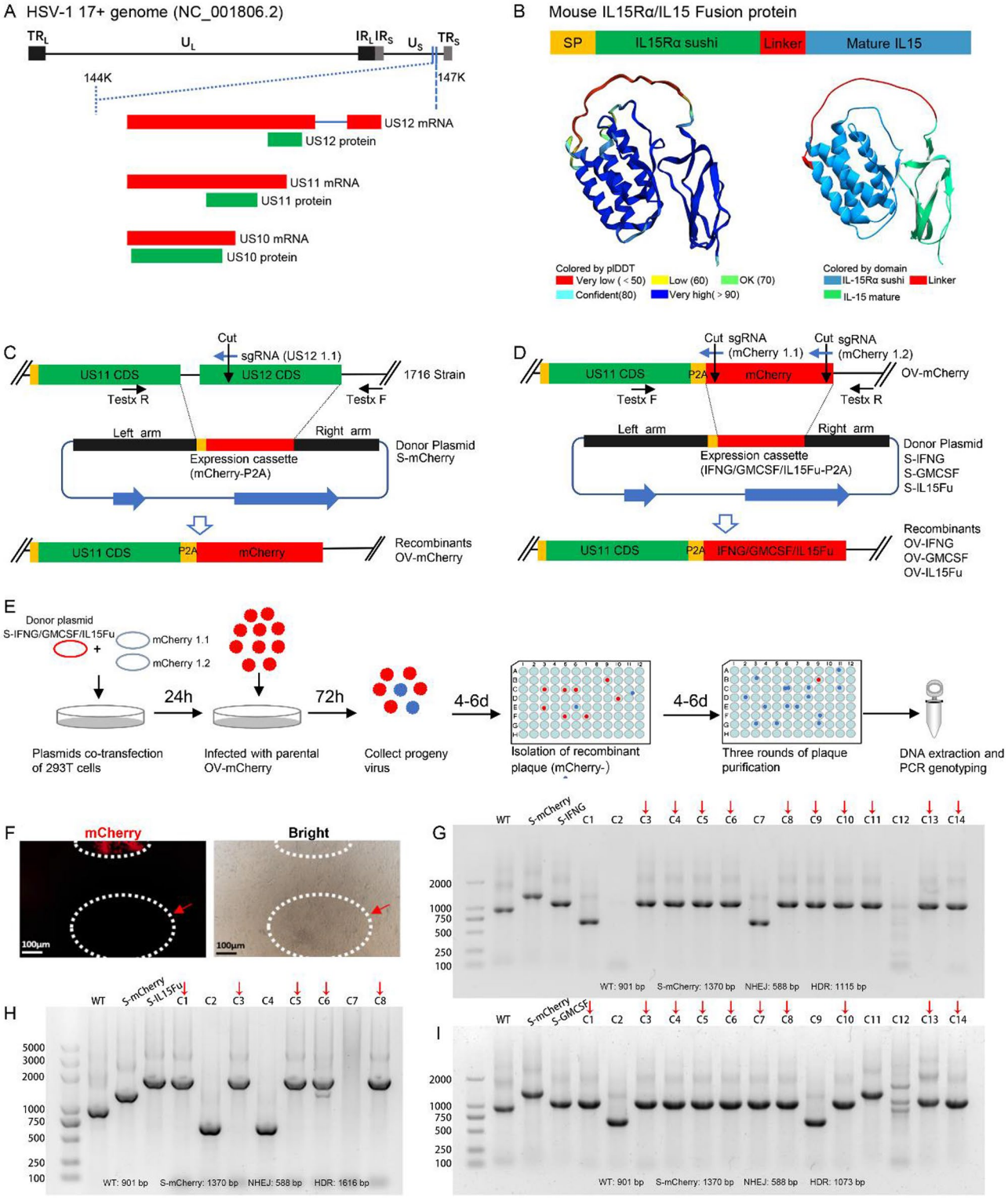

Fig. 1 (See legend on next page.)

presentation (TAP) then interfered with MHCI mediated immune response [15]. The majority of oncolytic HSV-1 strains have been genetically modified through deletion of ICP47 (encoded by US12 gene) to achieve higher activation of anti-tumor immunity. Based on the annotation of viral US12 locus of Human herpesvirus 1 strain 17 (NCBI Reference Sequence: NC_001806.2) (Fig. 1A), we design a platform to construct oncolytic

(See figure on previous page.)

Fig. 1 Cytokine-armed oncolytic virus construction based on CRISPR-Cas9 gene editing. **A** Schematic of US12 locus in Human herpesvirus 1 strain 17 (NCBI Reference Sequence: NC_001806.2). **B** The molecular construct of mouse IL15Rα/IL15 fusion protein. The three-dimensional model structures of this fusion proteins were predicted using AI-phaFold2 and colored by predicted Local-Distance Difference Test or different domain. **C-D** Schematic of CRISPR/Cas9-mediated HDR for replacing US12 with mCherry reporter gene (**C**) or replacing mCherry reporter with therapeutic cytokine genes (**D**) The target sites of gRNA (US12 1.1 or mCherry 1.1 + mCherry 1.2) were indicated by the black arrowhead. Primer pairs flanking the region of replacement were indicated by a black arrowhead. **E** Flowcharts of the gene editing of oncolytic HSV-1 genome and strategy for isolation of the potential recombinant virus (mCherry-). **F** Representative images of isolation of mCherry- recombinant virus after CRISPR/Cas9-mediated gene replacement. mCherry- recombinant virus clone was indicated by red arrowhead. Pictures were taken at 200X magnification, scale bars 100 μm. **G-I** PCR detection of NHEJ and HDR events in the mCherry- isolates in the construction of OV-IFNG (**G**), OV-IL15Fu (**H**) and OV-GMCSF (**I**), respectively. Potential isolates with target replacement (HDR) were indicated by red arrowhead

virus by accurately replacing the ICP47 coding sequence and the spacer region located directly upstream of US11 coding region with therapeutic gene and P2A sequence in the background of HSV-1 1716 strain. Theoretically, the therapeutic gene alone with the downstream gene US11, which is governed by late gene promoter, would be transcribed by the viral US12 immediate early promoter. Additionally, the early expression of US11 (α-expression) has been documented to augment viral replication in cancer cells [13].

To facilitate the isolation of recombinants, we designed a two-step strategy to generate oncolytic virus expressing GM-CSF, IFN-γ or IL15Rα/IL15 fusion protein on the back-ground of HSV-1 1716 strain. As depicted in Fig. 1B, the IL15Rα/IL15 fusion protein comprised interleukin-15 receptor alpha sushi domain linked by a 20-amino acid linker to the mature IL-15, which had been previously modified to significantly augment NK/$CD8^+$ T function [16].

Initially, the viral gene US12 was replaced with mCherry reporter gene with guide RNA targeting the US12 coding sequence. The resultant virus exhibited expression of mCherry-P2A-US11 under the US12 promoter, allowing for easy identification through the presence of red fluorescence, denoted as OV-mCherry (Fig. 1C). Subsequently, the mCherry reporter gene was exchanged with murine GM-CSF, IFN-γ, or IL15Fu. In order to enhance recombination efficiency, a pair of guide RNA sequences were designed to target both ends of the mCherry reporter gene, resulting in a precise cleavage following Cas9-mediated cleavage (Fig. 1D). As demonstrated in Fig. 1E, the progeny virus was harvested and subsequently introduced to Vero cells overlaid with DMEM medium supplemented with 1.5% methylcellulose. Putative recombinant virus (mCherry gene replaced with therapeutic gene) was identified through the absence of red fluorescence (Fig. 1E). Following purification of the recombinant virus genome DNA, a PCR analysis was conducted using primers flanking the US12 locus (TestxF/TestxR). As illustrated in Figs. 1G-I, the various editing events, such as non-homologous end joining (NHEJ) or homologous recombination repair (HDR), could be distinguished based on the size of the PCR products. Significantly, a majority of mCherry- mutants demonstrated successful integration of foreign genes via CRISPR-cas9 mediated HDR. The HDR rates for OV-IFNG, OV-GMCSF, and OV-IL15Fu were 71.4% (10/14), 71.4% (10/14), and 62.5% (5/8), respectively. In comparison to our previous method of inserting exogenous gene expression cassettes downstream of the LAP promoter in Exon 1 at the viral LAT locus, the efficiency of gene editing at the US12 locus, including exogenous gene insertion or replacement, was notably high and practical [17].

Characterization of oncolytic virus on cytokine expression and regulation of MHC antigen presentation in tumor cells

To confirm the exogenous gene expression mediated by oncolytic virus, supernatants from 4T1 tumor cells infected with various cytokine-armed oncolytic viruses were collected at 24 or 48-hours post-infection (hpi) for enzyme-linked immunosorbent assay (ELISA). As show in Fig. 2A-F, the expression levels of IFN-γ, GM-CSF and IL15Rα/IL15 fusion protein were notably elevated in the cells infected with OV-IFNG, OV-GMCSF and OV-IL15Fu, respectively. The infection of parental strain 1716 and oncolytic virus armed mCherry reporter gene (OV-mCherry) did not induce obvious expression of IFN-γ and IL15Rα/IL15 fusion protein. Of note, infection of 4T1 cells with OV-IFNG led to elevated levels of GM-CSF, comparable to those observed in OV-GMCSF infected cells.

As previously reported, the expression of MHCI and MHCII antigen presentation molecules can be regulated by pro-inflammatory cytokines. To investigate whether cytokine-armed oncolytic viruses influence antigen presentation, we evaluated the expression of MHCI and MHCII on tumor cells following infection. As shown in Fig. 2G, normal 4T1 cells exhibit constitutive MHCI expression. Although infection with OV-GMCSF and OV-IL15Fu resulted in increased MHCI expression on tumor cells, this increase was not statistically significant compared to OV-mCherry. Therefore, it is likely that the viral infection itself, rather than the cytokines, is responsible for the observed increase in MHCI expression, a well-documented response to viral infection. Similarly, for MHCII expression, both OV-GMCSF and OV-IL15fu failed to significantly increase MHCII expression when compared to the parental 1716 HSV or OV-mCherry

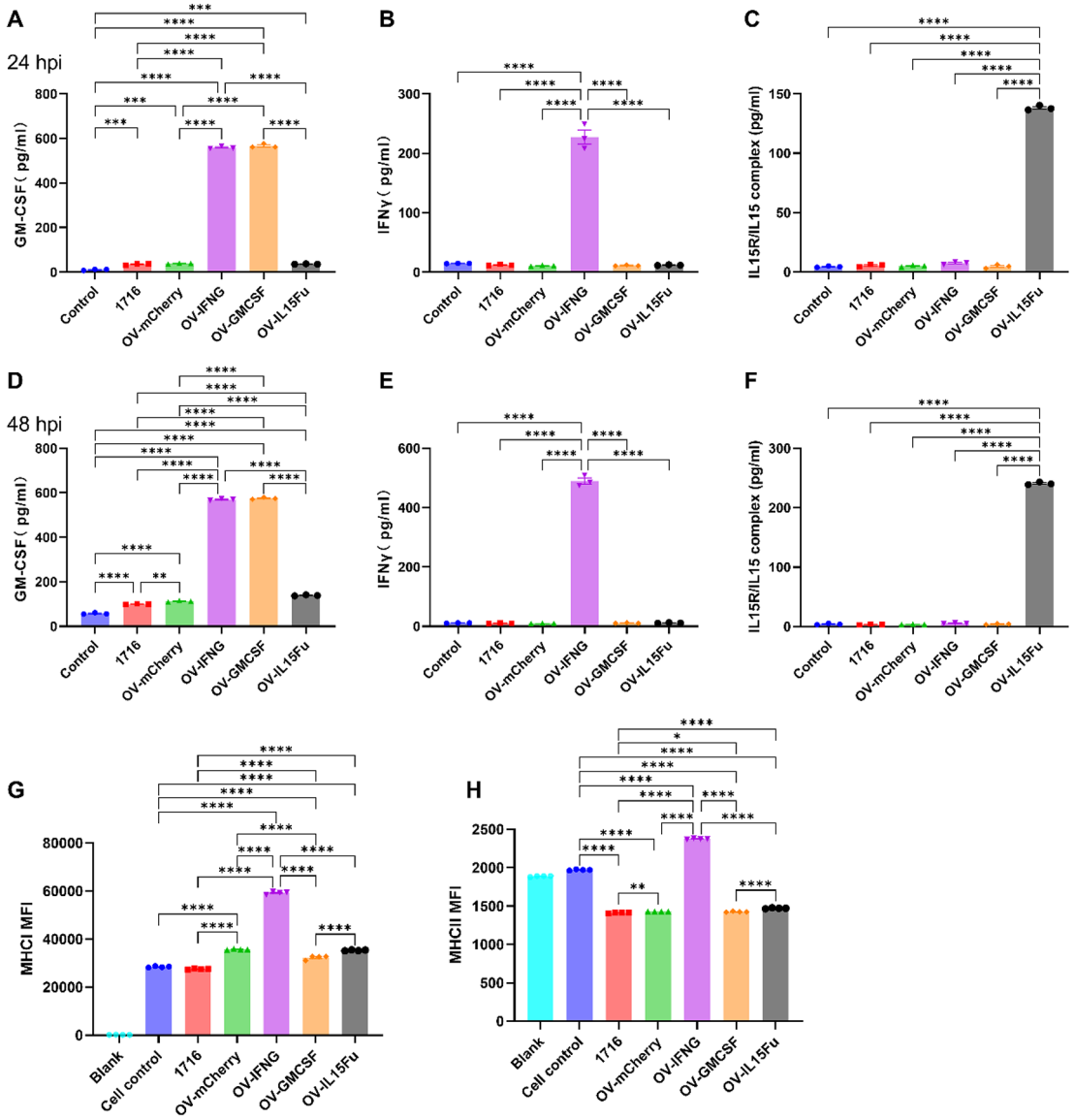

Fig. 2 Characterization of oncolytic viruses on cytokine expression and the regulation of MHC expression in tumor cells. **A-F** Expression of GM-CSF, IFN-γ and IL15Rα/IL15 fusion protein. 4T1 cells were infected with multiple strains of oncolytic HSV-1 at MOI = 1 for 24 h (**A**, **B**, **C**) or 48 h (**D**, **E**, **F**). Concentrations of indicated cytokines in supernatants were measured using conventional ELISA kits. Data are presented as mean ± SEM ($n = 3$), and statistical significance was calculated by one-way ANOVA followed by Bonferroni's multiple comparisons test. $^{**}p < 0.01$, $^{***}p < 0.001$, $^{****}p < 0.0001$. **G-H** MHCI and MHCII expression in 4T1 cells infected with various oncolytic HSV-1 strains. 4T1 cells were infected with oncolytic HSV-1 for 24 h at MOI = 1 then stained with fluorescent antibody against MHCI (**G**) or MHCII (**H**) and analyzed by flowcytometry. MFI, mean fluorescence intensity. Data are presented as mean ± SEM ($n = 4$), and statistical significance was calculated by one-way ANOVA followed by Bonferroni's multiple comparisons test. $^{****}p < 0.0001$

strains (Fig. 2H). Among the three cytokine-armed oncolytic HSV-1 constructs, only OV-IFNG significantly enhanced the expression of both MHCI and MHCII on tumor cells (Fig. 2G-H). This suggests that OV-IFNG may increase the immunogenicity of tumor cells through the substantial upregulation of both MHCI and MHCII molecules.

Cytopathic effect of oncolytic virus armed with cytokines in vitro

The oncolytic potential of cytokine-armed HSV-1 strains was evaluated across murine and human cancer models. In 4T1 TNBC cancer cells, the parental OV-mCherry strain demonstrated superior cytotoxicity compared to the original HSV-1 1716 strain (Fig. 3B), likely due to enhanced viral replication driven by early US11 expression. However, neither OV-IFNG nor OV-IL15Fu significantly improved cytotoxicity over OV-mCherry (Fig. 3A-B). In contrast, OV-GMCSF attenuated

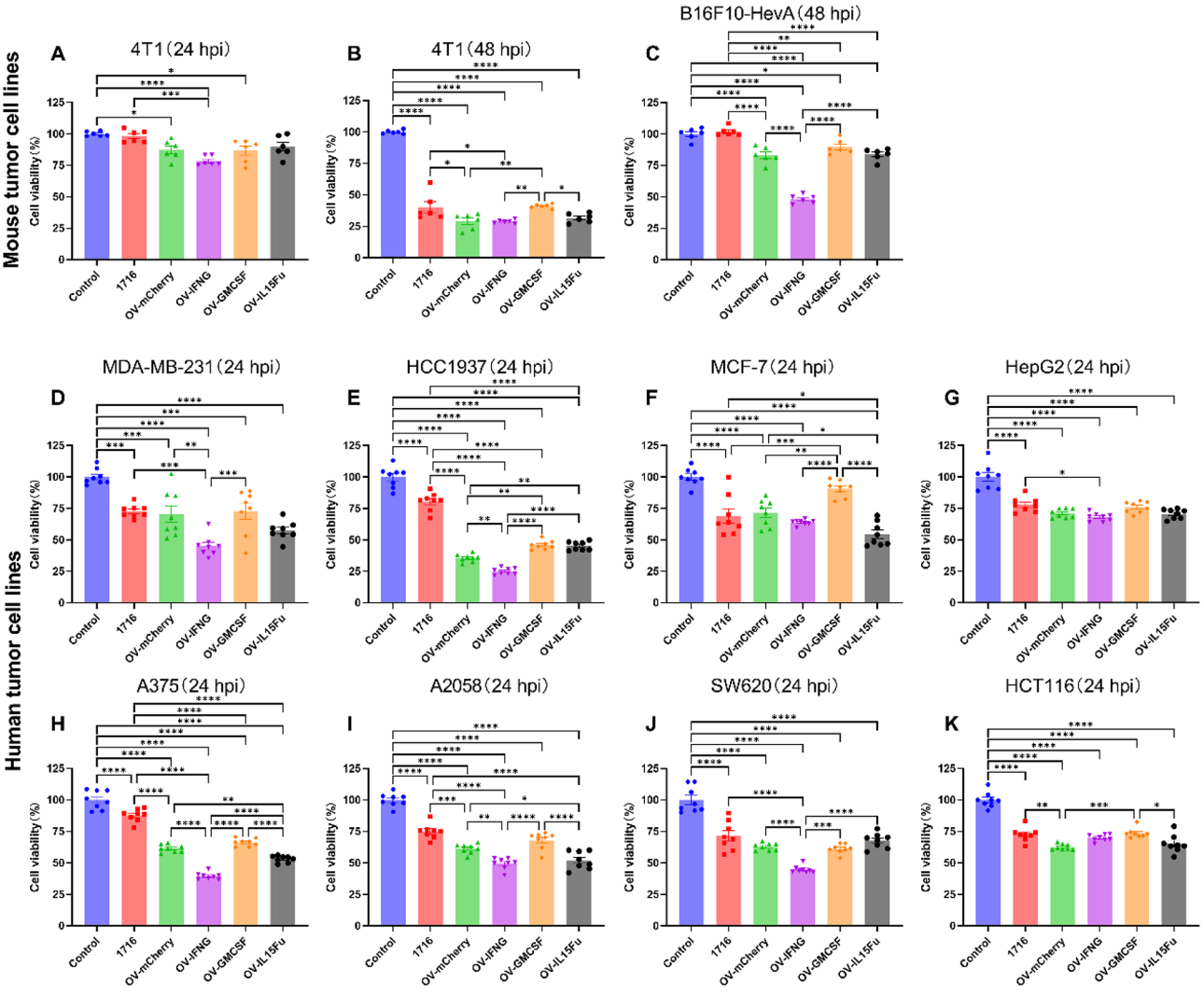

Fig. 3 Cytopathic effects of cytokine-armed oncolytic HSV1 strains in murine and human cancer cell lines. **A-B** Cytotoxicity of cytokine-armed oHSV1 strains against murine 4T1 triple-negative breast cancer cells infected at MOI 5 for 24 h (**A**) or 48 h (**B**). Cell viability was quantified using the CCK-8 assay. **C** Cytotoxicity against murine B16F10-mTNFRSF14 melanoma cells infected at MOI 100 for 48 h. **D-K** Cytotoxic activity in human cancer cell lines infected at MOI 5 for 24 h, including breast cancer (MDA-MB-231 [**D**], HCC1937 [**E**], MCF-7 [**F**]), hepatocellular carcinoma (HepG2 [**G**]), melanoma (A375 [**H**], A2058 [**I**]), and colon cancer (SW620 [**J**], HCT-116 [**K**]) cell lines. Data are presented as mean ± SEM. Statistical significance was analyzed by one-way ANOVA with Bonferroni's post hoc test (*$p < 0.05$, **$p < 0.01$, ***$p < 0.001$, ****$p < 0.0001$)

oncolytic efficacy in 4T1 cells at 48 h (Fig. 3B). In B16F10 melanoma models, despite overexpression of the HSV-1 entry receptor mTNFRSF14, parental oHSV1 strains showed limited cytotoxicity (Fig. 3C). Notably, OV-IFNG exhibited markedly enhanced oncolytic activity in B16F10-mTNFRSF14 cells compared to OV-mCherry and wild-type HSV-1 17+ (Fig. 3C). Real-time tracking of UL36-GFP expression confirmed that OV-IFNG achieved higher viral transcription and infection efficiency in this model (Supplementary Fig. 1).

Expanding to human cancer cell lines (MOI 5, 24 h), OV-IFNG showed selective cytotoxicity enhancement in MDA-MB-231 (breast), HCC1937 (breast), A375 (melanoma), A2058 (melanoma), and SW620 (colorectal) cells (Fig. 3D, E, H, I and J). Conversely, OV-GMCSF reduced cytotoxicity in HCC1937, MCF-7 (breast), and HCT116 (colorectal) cells (Fig. 3E, F and K), while OV-IL15Fu exhibited context-dependent effects—enhancing cytotoxicity in MCF-7 and melanoma lines but suppressing it in HCC1937 (Fig. 3F, H and I). qPCR profiling revealed cell line-specific cytokine receptor expression: GM-CSF receptors (*CSF2RA/CSF2RB*) were co-expressed only in HCC1937 and MDA-MB-231 cells, IFN-γ receptors (*IFNGR1/IFNGR2*) were ubiquitously detected, and IL-15 receptors (*IL2RB/IL2RG*) were co-expressed in breast cancer and melanoma lines (Supplementary Fig. 2). These observations suggest that cytokine payloads may modulate oncolytic activity through receptor-specific

interactions. For instance, IFN-γ's enhanced cytotoxicity in most receptor-positive lines (*IFNGR1/IFNGR2*$^+$) could stem from its immunogenic effects, while GM-CSF's attenuated activity in *CSF2RA/CSF2RB*$^+$ cells might reflect immune-independent protumor pathways [18–20]. However, these mechanisms remain speculative and require further validation.

Evaluation of the antitumor efficiency of oncolytic virus in murine mammary cancer mode

The anti-tumor activity of cytokine-armed oncolytic virus was further assessed in a 4T1 syngeneic mammary tumor model. Tumor-bearing mice were intratumorally injected with 10^7 PFU indicated virus or the same volume of PBS (summarized in Fig. 4A). Compared with the control group, all oncolytic strains, including the parental strain 1716, demonstrated a certain degree of tumor growth inhibition (Fig. 4B). However, none of the cytokine-loaded oncolytic strains exhibited significantly greater tumor inhibitory effects than the background strain OV-mCherry, indicating that the expression of these cytokines had minimal impact on the antitumor efficacy of oncolytic viruses (Fig. 4B). At 24 days following the initial treatment, the tumor volume in the OV-mCherry treated group exhibited a slight reduction (not significant) compared to that of the HSV-1 1716 treated groups, suggesting that the absence of viral US12 and the early expression of US11 may enhance the anti-tumor efficacy of HSV-1 (Fig. 4C). While in the survival analysis, mice treated with OV-IL15fu exhibited a significantly prolonged survival compared to other cytokine-loaded strains (OV-GMCSF and OV-IFNG) and the background strain (OV-mCherry) (Fig. 4D). Overall, OV-IL15fu demonstrated superior therapeutic outcomes in a murine 4T1 breast cancer model.

Notably, treatment with OV-IFNG led to a significant mortality rate of 37.5% (3 out of 8) during the early stages of treatment (Fig. 4D), suggesting a severe cytokine-mediated systemic toxicity. It was noteworthy that the OV-IL15Fu significantly prolonged the survival of tumor-bearing mice compared to other viruses. While GM-CSF is commonly utilized to enhance the immunomodulatory

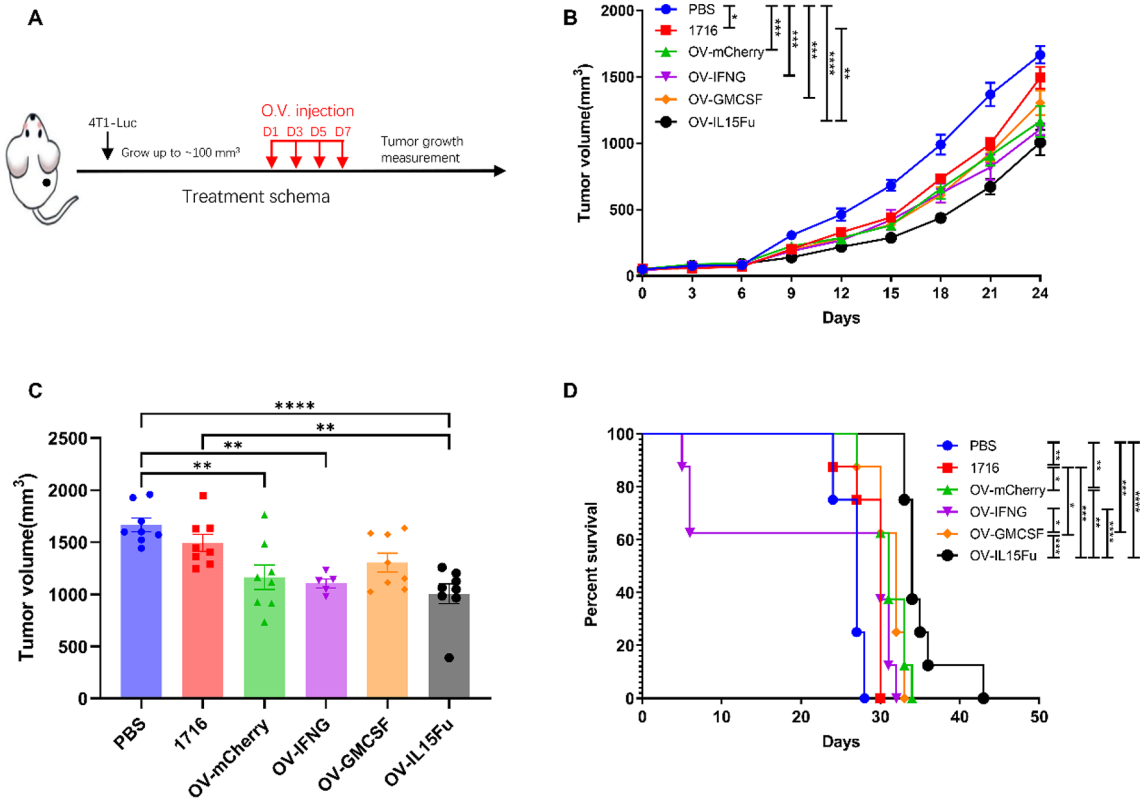

Fig. 4 Antitumor effects of cytokine-armed oncolytic HSV-1 in 4T1 mammary tumor model. **A** Schematic of BALB/c mice with subcutaneous 4T1 tumors treated with oncolytic virus. When tumor sizes reached ~ 100 mm^3 (designated as Day 1), the mice were intratumorally injected 1×10^7 PFU oncolytic HSV-1 or the same volume of PBS at days 1, 3, 5, 7 (red arrowheads). The tumor growth was monitored with caliper measurement every three days. **B** Kaplan–Meier survival curve of tumor bearing mice treated with oncolytic virus ($n = 8$ mice). The statistical differences between groups were determined using two-tailed log rank (Mantel-Cox) test. *$P < 0.05$, **$p < 0.01$, ***$p < 0.001$, ****$p < 0.0001$. **C** Tumor growth curves for all treatment groups in the 4T1 tumor model. Data presented as the means ± SEM ($n = 8$). The statistical differences between groups were determined by two-way ANOVA with multiple comparisons. *$p < 0.05$, **$p < 0.01$, ***$p < 0.001$ and ****$p < 0.0001$. **D** Tumor volume of treated mice on day 24. Data presented as the means ± SEM. Statistical significance was calculated by one-way ANOVA followed by Bonferroni's multiple comparisons test. ****$p < 0.0001$

capabilities of oncolytic viruses, our findings indicate that it may not effectively enhance anti-tumor efficacy in the murine 4T1 TNBC model.

Cytokine-armed oncolytic virus distinctively modulation antitumor immunity reveled by RNA sequencing

To further explore the antitumor immune response induced by cytokine-armed oncolytic viruses in 4T1 mammary tumors, gene expression analysis was performed on tumors treated with various HSV-1 strains 14 days post initial treatment. A comparison of the transcriptome between the OV-mCherry treatment group and mock treated tumors revealed a notable increase in the expression of genes associated with immune activation pathways, including cytokine-related signaling pathways and the innate NF-κB signaling pathway, suggesting a pro-inflammatory modulation of oncolytic virus infection (Fig. 5A). Furthermore, the oncolytic virus armed with GM-CSF was found to enhance cytokine/chemokine signaling pathways, as well as myeloid leukocyte migration and cell chemotaxis pathways, potentially through direct positive regulation by GM-CSF (Fig. 5D). Surprisingly, treatment with OV-GMCSF resulted in a significant inhibition of antigen processing and presentation pathways, as evidenced by the downregulation of several genes related to MHCI and MHCII pathways (Fig. 5E, F). This observation may offer insight into the lack of enhanced anti-tumor effects observed with OV-GMCSF compared to the control virus OV-mCherry in the 4T1 tumor model. While the OV-IFNG demonstrated a notably high mortality rate in treating 4T1 tumors in vivo, potentially attributed to the cytokine toxicity of IFN-γ, its inoculation has been shown to enhance immune activation-related signaling pathways, such as cytokine/chemokine signaling pathways, regulation of T cell activation, and leukocyte migration (Fig. 5G, H and I). In contrast, the oncolytic virus expressing IL15Rα/IL15 fusion proteins selectively upregulated pathways associated with T cell activation and natural killer cell-mediated cytotoxicity, in addition to cytokine/chemokine signaling pathways (Fig. 5B, C). Together, these findings indicated that the cytokine produced by oncolytic virus may play a vital role in orchestrating the anti-tumor immunity. Nonetheless, caution should be exercised in selecting cytokines as immunomodulatory genes for oncolytic therapy, taking into account potential cytotoxic effects and the heterogeneity of cancer.

Flow cytometry analysis revealed distinct Immunomodulatory profiles induced by cytokine-armed oncolytic virus

To delineate the immunomodulatory effects of cytokine-expressing oHSV1 in 4T1 triple-negative breast tumors, we quantified effector molecule expression (IFN-γ and GZMB) in tumor-infiltrating and splenic lymphocytes and characterized myeloid subsets critical for antigen presentation and immune regulation.

Among tumor-infiltrating lymphocytes, OV-IL15Fu elicited the most robust cytotoxic response, elevating GZMB expression in $CD8^+$ T cells by 2.13-fold compared to PBS and 1.44-fold over OV-IFNG (Fig. 6K). In contrast, OV-IFNG preferentially activated $CD4^+$ T cells and NK cells, significantly increasing IFN-γ^+CD4^+ T cells (1.66-fold vs. PBS, Fig. 6J) and $GZMB^+$ NK cells (1.66-fold vs. PBS, Fig. 6M), consistent with IFN-γ's established role in Th1 polarization and innate immune activation [21]. However, OV-IFNG exhibited limited efficacy in driving $CD8^+$ T cell cytotoxicity (Fig. 6K), suggesting a functional trade-off between systemic immune priming and localized effector responses. Strikingly, OV-GMCSF failed to enhance IFN-γ or GZMB expression across T and NK cell subsets, mirroring the empty vector OV-mCherry or PBS control (Fig. 6I-N), a paradox potentially linked to compensatory immunosuppressive pathways counteracting GM-CSF's adjuvant potential [22]. In the spleen, both OV-IFNG and OV-IL15 modestly upregulated GZMB in $CD8^+$ T and NK cells (Fig. 6E, G), while OV-GMCSF uniquely suppressed splenic NK cell activation compared to OV-mCherry (Fig. 6G), indicative of systemic immune tolerance.

Concurrently, all oHSV1 strains—including the control OV-mCherry—provoked profound shifts in tumor-associated myeloid populations. M1 macrophages ($CD45^+F4/80^+CD11c^-MHCII^+$) were reduced across treatment groups, while M2 macrophages ($CD45^+F4/80^+CD11c^-MHCII^-$) expanded, culminating in a diminished M1/M2 ratio (Fig. 7B-C, H). It could be speculated that the HSV1induced STING pathway may promote TAMs polarization to anti-inflammatory M2 phenotypes [23, 24]. Notably, all the oHSV1 strains, except OV-GMCSF, amplified infiltration of PMN-MDSCs ($CD45^+CD11b^+Ly6G^+$). The m-MDSCs ($CD45^+CD11b^+Ly6C^+Ly6G^-$) and patrolling monocytes ($CD45^+CD11b^+Ly6C^-Ly6G^-$), which exhibit context-dependent antitumor or immunosuppressive roles [25], also increased in OV-IFNG and OV-IL15Fu treated groups. Paradoxically, OV-GMCSF slightly enriched $MHCII^+$ subsets within cDCs, m-MDSCs, and patrolling monocytes compared to the OV-IL15Fu (Fig. 7D-F), reflecting GM-CSF's dual capacity to drive myeloid maturation while preserving partial immunosuppressive features [26].

Together, these myeloid shifts underscore a microenvironmental paradox: despite divergent T/NK cell responses, all oHSV1 strains exacerbated immunosuppressive networks. PMN-MDSCs, known to inhibit $CD8^+$ T cells via ROS and arginase-1 [27, 28], likely attenuated OV-IL15Fu's cytotoxic potential, while

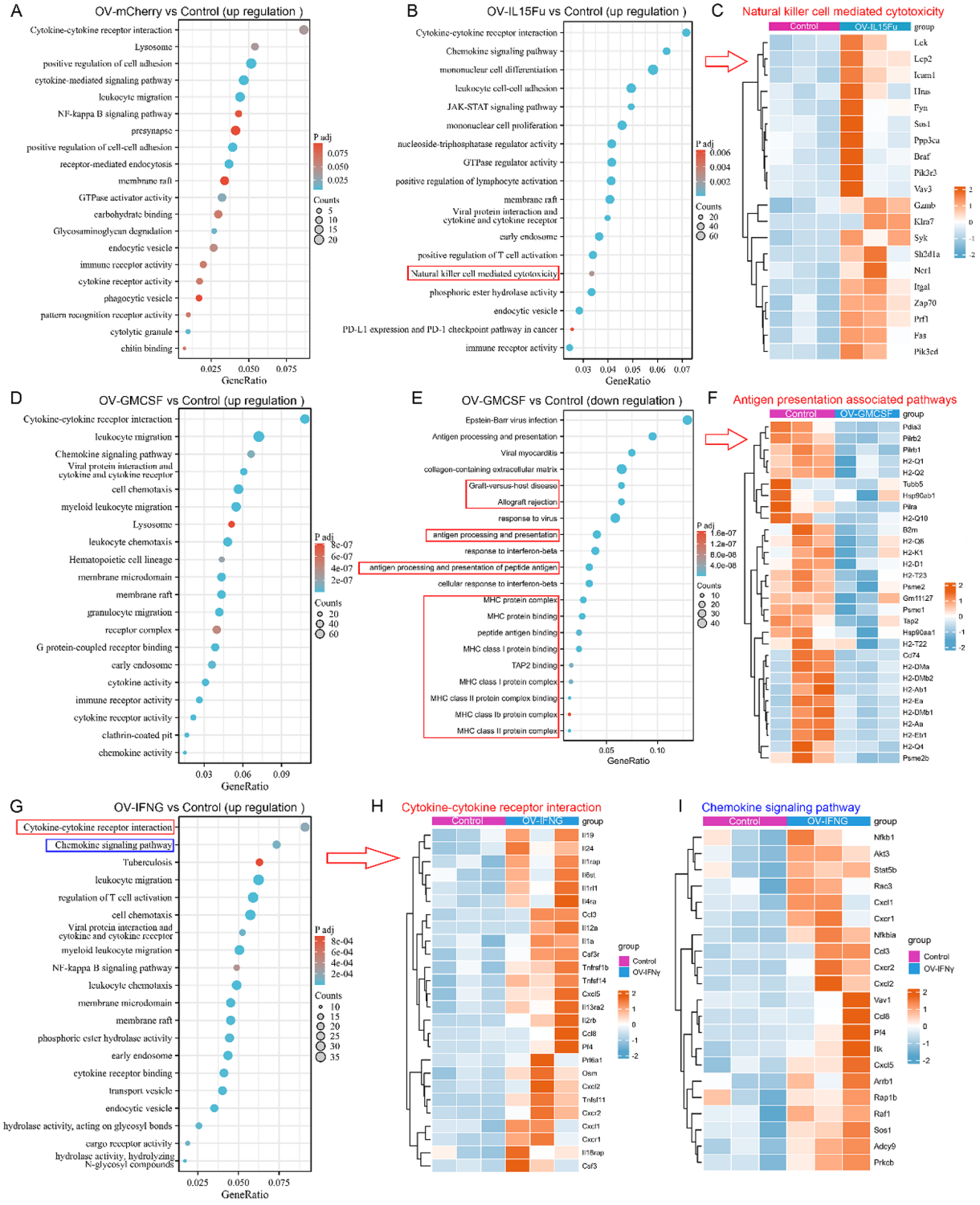

Fig. 5 Transcriptome analysis of 4T1 tumors treated with cytokine-armed oncolytic virus. **A** KEGG pathway enrichment analysis of upregulated DEGs between the OV-mCherry treatment and control groups. **B** KEGG pathway enrichment analysis of upregulated DEGs between the OV-IL15Fu treatment and control groups. Red boxes indicate the enrichment of natural killer cell mediated cytotoxicity. **C** Heatmap of differentially expressed genes enriched in the natural killer cell mediated cytotoxicity pathway. **D-E** KEGG pathway enrichment analysis of upregulated (**D**) and downregulated (**E**) DEGs between the OV-GMCSF treatment and control groups. Red boxes indicate the enrichment of antigen processing and presentation associated pathways. **F** Heatmap of differentially expressed genes enriched in antigen processing and presentation associated pathways. **G** KEGG pathway enrichment analysis of upregulated DEGs between the OV-IFNG treatment and control groups. **H-I** Heatmap of differentially expressed genes enriched in the cytokine-cytokine receptor interaction pathway (**H**) and chemokine signaling pathway (**I**)

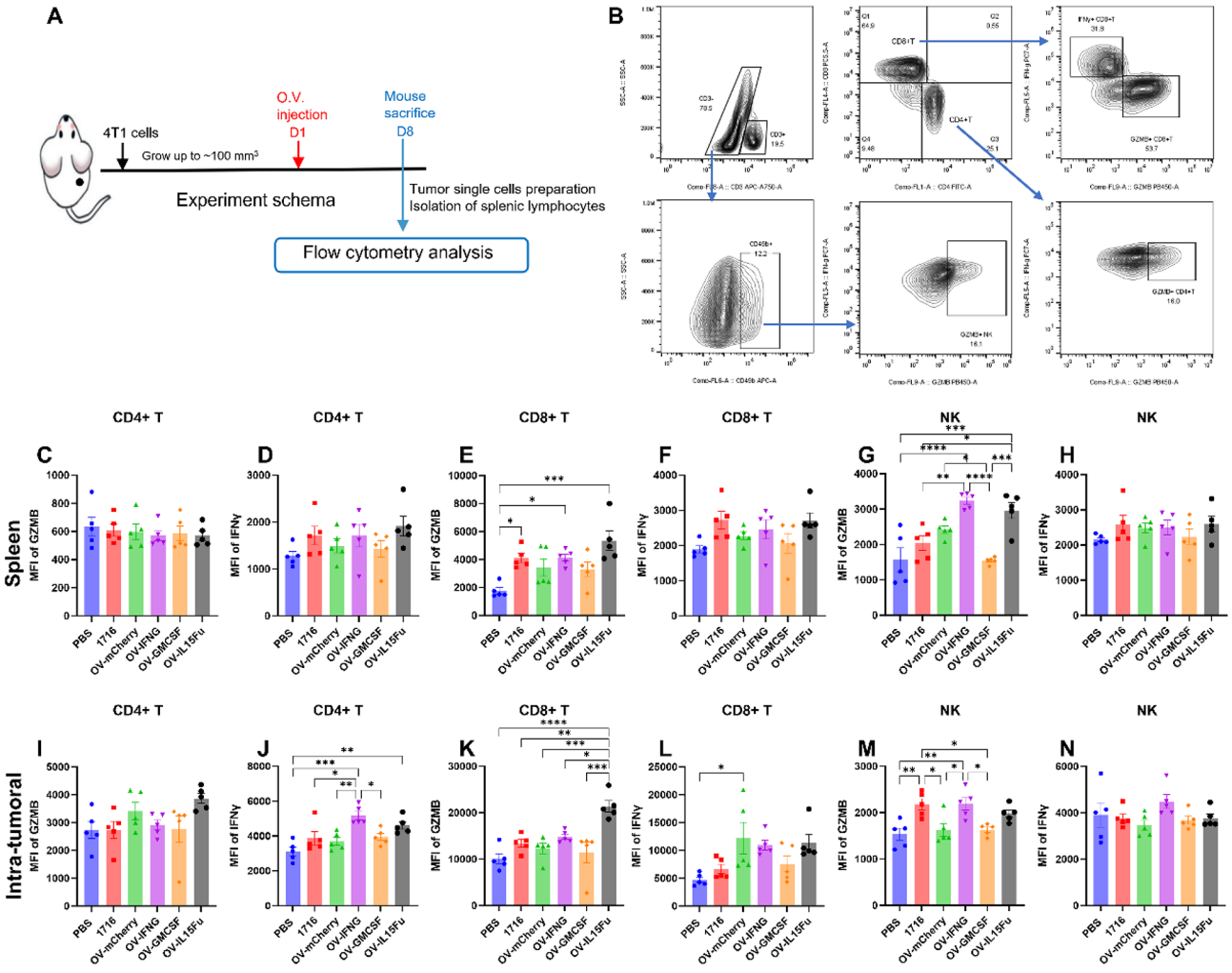

Fig. 6 Cytokine-armed oncolytic virus modulates tumor immunity via T/NK effector response. **A** Schematic of BALB/c mice with subcutaneous 4T1 tumors treated with oncolytic virus. One week post intratumoral injection of OVs (10^7 PFU), the mice in each group ($n = 5$) were sacrificed, the tumoral single cells and splenic lymphocytes were stained with live-dead dye and fluorescent antibodies. **B** Representative flow cytometry plots for intracellular staining of GZMB, IFN-γ in $CD4^+$, $CD8^+$, and NK($CD49b^+$) cells. The single cell suspension was subjected to live dead staining and live single cells were gated for further analysis. **C-N** The mean fluorescence intensity (MFI) of GZMB and IFN-γ on spleen(**C**-**H**) or tumoral $CD4^+$T, $CD8^+$T and NK cells. Data presented as the means ± SD. Statistical significance were calculated by one-way ANOVA followed by Bonferroni's multiple comparisons test. $^*p < 0.05$, $^{**}p < 0.01$, $^{***}p < 0.001$ and $^{****}p < 0.0001$

m-MDSCs—differentiated from inflammatory monocytes via CCL2/CCR2 signaling in breast cancer [29]—may have blunted OV-IFNG's Th1 polarization through TGF-β-mediated Treg induction [30]. The selective $MHCII^+$ enrichment by OV-GMCSF, though indicative of antigen-presenting cell maturation, highlights the challenge of overcoming entrenched immunosuppression in advanced 4T1 tumors, where myeloid plasticity often subverts therapeutic intent.

Discussion

A comprehensive comprehension of the genetic mechanisms of viruses is crucial for im-proving oncolytic viruses (OVs) as a vector for therapeutic purposes. Although the deletion or mutation of genes in the creation of oHSV1 can enhance its selectivity, it may also diminish its tumor lysis capabilities. Consequently, current research is focused on integrating the advantageous features to explore various potential therapeutic options, such as cytokines, chemokines, immune checkpoint inhibitors, co-stimulatory ligands, and antibodies [31].

OVs engineered to express and secrete GM-CSF have been developed with the aim of promoting DCs maturation and enhancing monocyte/macrophage activity, ultimately leading to improved local presentation of tumor antigens and eliciting antigen-specific T cell responses [32–34]. However, the results of this study, in conjunction with other relevant research, suggest that the influence of GM-CSF on tumor progression may be predominantly dependent on the specific type of tumor.

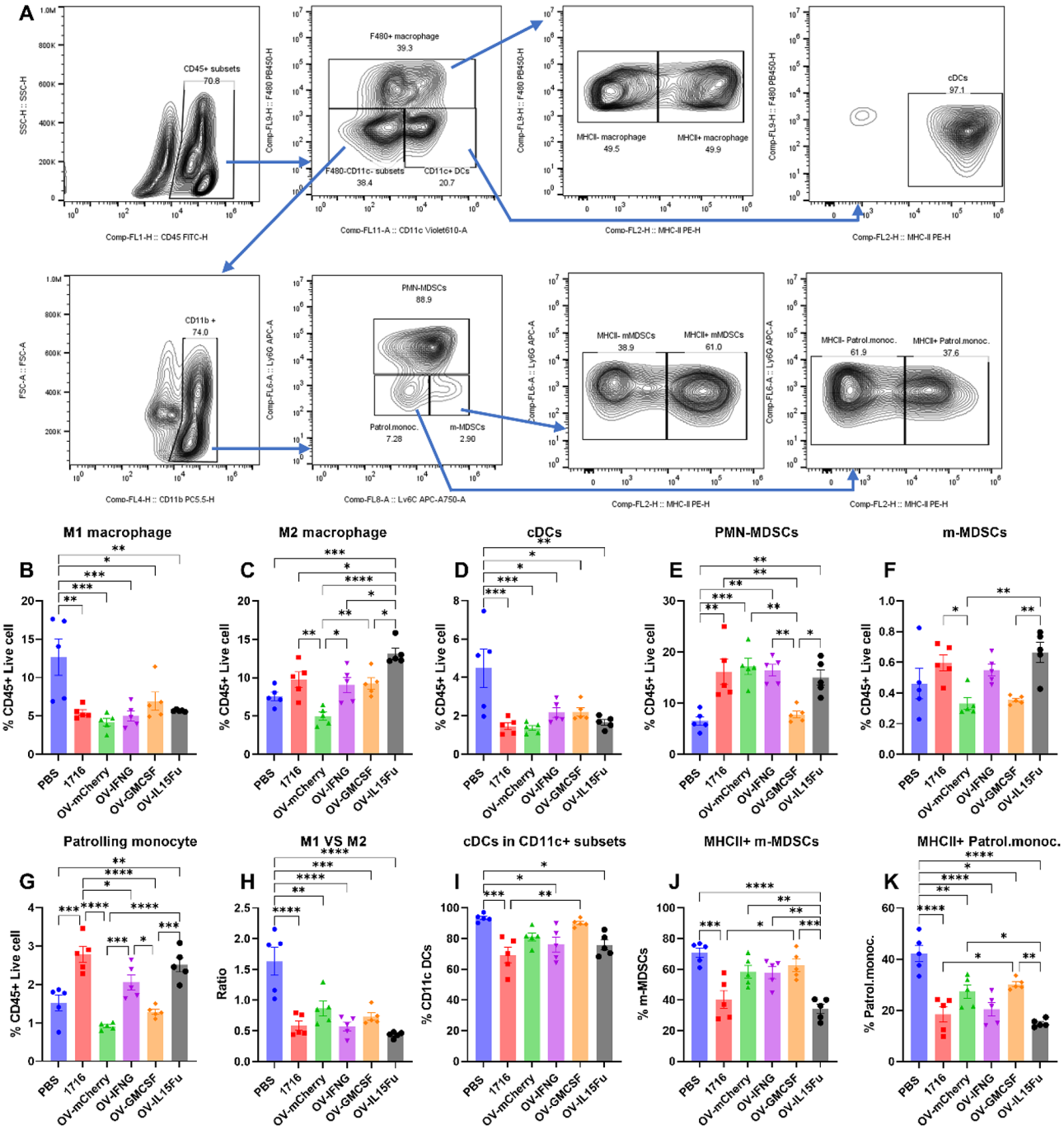

Fig. 7 Cytokine-armed oncolytic virus remodel the intra-tumoral myeloid compartment. **A** Gating strategy. The single cell suspension was subjected to live dead staining and live CD45 cells were gated for further identifing and quantification the cell population of $MHCII^{+}$ (M1) macrophages (**B**), $MHCII^{-}$ (M2) macrophages (**C**), cDCs(**D**), PMN-MDSCs (**E**), m-MDSCs (**F**), patrolling monocytes (**G**). The ratio of M1 to M2 macrophages (**H**) and the percentage of MHCII + subsets in CD11c + DCs(**I**), m-MDSCs (**J**) and patrolling monocytes (**K**) were also calculated. Data presented as the means ± SD. Statistical significance was calculated by one-way ANOVA followed by Bonferroni's multiple comparisons test. *$p < 0.05$, **$p < 0.01$, ***$p < 0.001$ and ****$p < 0.0001$

Although GM-CSF has been commonly utilized as an adjuvant in cancer immunotherapy, numerous studies have demonstrated that GM-CSF can actually facilitate tumor growth via both immune-dependent and independent mechanisms. Constitutive expression of GM-CSF and its receptors has been identified in various types of cancer, including gliomas [18], skin carcinoma [35], meningiomas [36] and head and neck cancer [37]. Additionally, GM-CSF has been demonstrated to enhance cancer cell proliferation and migration in vitro through

immune-independent mechanisms, potentially involving the activation of STAT5 and MERK [18, 35]. Furthermore, GM-CSF contributes to the advancement of cancer by facilitating the production of tumor-associated macrophages and myeloid-derived suppressor cells. In breast tumors, GM-CSF derived from tumor cells accelerates tumor progression by inducing a substantial increase in ARG1-expressing myeloid cells through STAT3 and p38 MAPK signaling pathways [22]. In Epstein-Barr virus-associated nasopharyngeal carcinoma, tumor cell-derived GM-CSF promotes metastasis by attracting and activating macrophages [38].

Despite demonstrating clinical efficacy in melanoma (T-VEC) [8], GM-CSF-armed HSV1 failed to confer survival benefits in our 4T1 TNBC murine model (Fig. 4). Integrated RNA sequencing and flow cytometry analyses revealed multifaceted immunomodulatory effects: OV-GMCSF downregulated antigen presentation pathways (Fig. 5E-F), showed no significant enhancement of T cell or NK cell activation markers (Fig. 6), and paradoxically promoted myeloid cell maturation (Fig. 7). These findings suggest that in the immune-suppressive microenvironment of TNBC, GM-CSF may preferentially drive STAT3/p38 MAPK-mediated expansion of $ARG1^+$ MDSCs, overriding its potential to enhance antigen presentation—an effect previously observed in murine and human breast cancer models [39, 40]. This may help explain the lack of therapeutic benefit in our study, particularly in contrast with melanoma, where GM-CSF has shown efficacy likely due to its lymphocyte-rich microenvironment and lower MDSC content. Our findings highlight the context-dependent performance of GM-CSF in oHSV therapy and underscore the importance of tumor-specific cytokine selection rather than extrapolating from other tumor models.

While IFNs has traditionally been considered a key element in anti-tumor immunity, its systemic toxicities and short half-life post-administration constrain its overall bioavailability. The oncolytic vesicular stomatitis virus (VSV) [41] or adenovirus [42] encoding IFN-γ demonstrated improved anti-tumor efficacy by inducing selective oncolysis and immune response activation. Conversely, IFN-β-armed VSV displayed adverse effects in patients but was deemed safe in healthy individuals during a phase I clinical trial [43]. In our study, IFN-γ was included not as a candidate therapeutic payload, but as a mechanistic comparator to evaluate immune activation relative to other cytokines. This rationale was based on its well-established immunostimulatory effects and its mechanistic overlap with IL-12, which we deliberately avoided to prevent interpretive redundancy.

Furthermore, our findings demonstrate that OV-IFNG amplified MHC expression (Fig. 2G-H) and Th1 polarization (Fig. 6J) but induced early mortality (Fig. 4D) linked to systemic IFN-γ toxicity. Notably, IFN-γ's expansion of PMN-MDSCs (Fig. 7B) likely counteracted its immunogenic effects.These results align with prior reports that excessive IFN-γ signaling can paradoxically suppress antitumor immunity by inducing $CD4^+$ T cell depletion and increasing myeloid-driven immunosuppression [44]. Altogether, while IFN-γ exerts potent immunological effects, its narrow therapeutic window and risk of systemic toxicity limit its translational potential in this context.

In contrast to the majority of cytokines which act through paracrine and autocrine, interleukin-15 (IL-15) is expressed and trans-presented in conjunction with its high affinity receptor IL-15 Rα on the surface of IL-15-producing cells [45]. This allows IL-15 to transmit signals to target cells expressing IL-2 Rβ/γ receptor subunits, leading to activation of JAK-STAT signaling pathway [46]. IL-15 plays a crucial role in stimulating the proliferation and activation of NK cell, natural killer T cell, and $CD8^+$ T cells, particularly memory phenotype $CD8^+$ T cells, resulting in enhanced cytotoxicity and the pro-duction of IFN-γ and IFN-α [47]. Furthermore, IL-15 exerts an inhibitory effect on the apoptosis of immune cells by upregulating the expression of anti-apoptotic proteins and downregulating the production of pro-apoptotic proteins [48]. In this research, oncolytic HSV-1 was utilized to express a fusion protein consisting of the IL-15 Rα sushi domain linked to the mature form of IL15, known as RLI. This fusion protein demonstrated potent anticancer activity in metastatic melanoma and colorectal cancer models [16]. Consistent with these findings, our study showed that OV-IL15Fu achieved superior survival benefit in the aggressive 4T1 model, despite its known resistance to immunotherapy. Although the survival extension was modest (~2–3 days), this outcome is notable given the 4T1 model's low immunogenicity and high MDSC burden. Prior oHSV studies in 4T1—including IL-12-armed variants—have similarly shown only modest improvements, further supporting our conclusion that OV-IL15Fu confers biologically meaningful benefit in a stringent setting [49]. Importantly, this benefit was achieved without systemic toxicity, differentiating IL-15Fu from IFN-γ and suggesting translational potential in TNBC.

In addition, the effectiveness of virotherapy treatment may also rely on maintaining balance between the host's the anti-tumor immunity and the antiviral response induced by oncolytic viruses. Upon infection, the host's immune system is triggered to restrict viral spread and facilitate viral eradication, which may compromise the therapeutic benefits. Recent studies have shown that oncolytic viruses such as T-VEC often replicate only transiently after intratumoral injection, with rapid immune-mediated clearance [50]. However, this

initial burst of lysis is sufficient to trigger immunogenic tumor cell death and initiate systemic immune responses [51, 52]. This underscores the paradigm shift in which oncolytic viruses are increasingly recognized as immune primers rather than direct cytolytic agents. Researchers have developed various strategies, such as chemical polymers [53], liposomes [54, 55], and protective coatings [56, 57], to protect oncolytic viruses from neutralizing antibody binding. An alternative approach involves using cellular carriers loaded with oncolytic viruses to shield them from immune-mediated factors [58, 59]. Nonetheless, arming oncolytic viruses with cytokines such as IL-15Fu remains a compelling strategy to locally modulate the tumor microenvironment and enhance immune engagement in tumors that are otherwise unresponsive.

Conclusions

In summary, we have developed a platform for highly efficient construction of oncolytic HSV-1 through CRISPR/Cas9 mediated homologous recombination. Our platform can be expanded to express other therapeutic genes, thereby enhancing the efficacy of oncolytic virotherapy. This study provides the first head-to-head comparison of cytokine-armed oHSV1 in TNBC, revealing context-dependent benefits and limitations of IFN-γ, GM-CSF, and IL15Fu. Our findings inform rational cytokine selection for clinical oHSV1 development, emphasizing the need to tailor immunomodulatory payloads to tumor-specific immune landscapes.

Abbreviations

DCs	Dendritic cells
ELISA	Enzyme-linked immunosorbent assay
GM-CSF	Granulocyte-macrophage colony-stimulating factor
HDR	Homologous recombination repair; hpi: hours post-infection
IL-15	Interleukin-15
IL15Fu	IL-15Rα/IL-15 fusion protein
MDSCs	Myeloid-derived suppressor cells
NHEJ	Non-homologous end joining
oHSV1	Oncolytic herpes simplex virus type 1
OVs	Oncolytic viruses
TAP	Transporter associated with antigen presentation
TILs	Tumor-infiltrating lymphocytes
TME	Tumor microenvironment
TNBC	Triple-negative breast cancer
VSV	Vesicular stomatitis virus

Supplementary Information

The online version contains supplementary material available at https://doi.org/10.1186/s12985-025-02758-y.

Supplementary Material 1

Acknowledgements

We are grateful to Professor Nigel William Fraser from the University of Pennsylvania for HSV-1 1716 Virus.

Author contributions

Conceptualization, Y.G., Y.Z., P.W. and X.H.; methodology, Y.G., C.W., Y.Z. and J.T.; formal analysis, Y.G., Y.Z., Z.N. and J.Y.; data curation, P.W. and X.H.; writing—original draft preparation, Y.G.; writing—review and editing, X.H.; visualization, Y.G., C.W. and X.H.; supervision, P.W. and X.H.; All authors have read and agreed to the published version of the manuscript.

Funding

This research was funded by National Natural Science Foundation of China (grant no. 82260486), Yunnan Revitalization Talent Support Program, and the Medical Reserve Talents Training Plan of Yunnan Province (grant no: H-2019059).

Data availability

No datasets were generated or analysed during the current study.

Declarations

Ethics approval and consent to participate

All animal experiments were performed in accordance with the ethical review standards set by the Ethical Review Committee of the Laboratory Animal Department at Kunming Medical University.

Consent for publication

Not applicable.

Competing interests

The authors declare no competing interests.

Author details

[1]Kunming Medical University, Kunming, Yunnan, China
[2]Key Laboratory of The Second Affiliated Hospital of Kunming Medical University, Kunming, Yunnan, China

Received: 20 March 2024 / Accepted: 22 April 2025
Published online: 05 May 2025

References

1. Lehmann BD, et al. Identification of human triple-negative breast cancer subtypes and preclinical models for selection of targeted therapies. J Clin Investig. 2011;121(7):2750–67.
2. Bianchini G, et al. Triple-negative breast cancer: challenges and opportunities of a heterogeneous disease. Nat Reviews Clin Oncol. 2016;13(11):674–90.
3. Kaufman HL, Kohlhapp FJ, Zloza A. Oncolytic viruses: a new class of immunotherapy drugs. Nat Rev Drug Discovery. 2015;14(9):642–62.
4. Lawler SE, et al. Oncolytic viruses in cancer treatment: a review. JAMA Oncol. 2017;3(6):841–9.
5. Leonard JP, et al. Effects of single-dose interleukin-12 exposure on interleukin-12–associated toxicity and interferon-γ production. Blood J Am Soc Hematol. 1997;90(7):2541–8.
6. Lasek W, Zagożdżon R, Jakobisiak M. Interleukin 12: still a promising candidate for tumor immunotherapy? Cancer Immunol Immunother. 2014;63:419–35.
7. Beatty GL, Paterson Y. IFN-γ-dependent Inhibition of tumor angiogenesis by tumor-infiltrating CD4 + T cells requires tumor responsiveness to IFN-γ. J Immunol. 2001;166(4):2276–82.
8. Andtbacka RH, et al. Talimogene Laherparepvec improves durable response rate in patients with advanced melanoma. J Clin Oncol. 2015;33(25):2780–8.
9. Highfill S.L., et al. Disruption of CXCR2-mediated MDSC tumor trafficking enhances anti-PD1 efficacy. Sci Transl Med. 2014;6(237):ra23767–23767.
10. Waldmann TA. The biology of interleukin-2 and interleukin-15: implications for cancer therapy and vaccine design. Nat Rev Immunol. 2006;6(8):595–601.
11. Chaurasiya S, Fong Y, Warner SG. Optimizing oncolytic viral design to enhance antitumor efficacy: progress and challenges. Cancers. 2020;12(6):1699.
12. Bi Y, et al. High-efficiency targeted editing of large viral genomes by RNA-guided nucleases. PLoS Pathog. 2014;10(5):e1004090.
13. Todo T, et al. Oncolytic herpes simplex virus vector with enhanced MHC class I presentation and tumor cell killing. Proc Natl Acad Sci U S A. 2001;98(11):6396–401.
14. Selvanesan BC, et al. NSC243928 treatment induces anti-tumor immune response in mouse mammary tumor models. Cancers. 2023;15(5):1468.

15. Neumann L, et al. The active domain of the herpes simplex virus protein ICP47: a potent inhibitor of the transporter associated with antigen processing. J Mol Biol. 1997;272(4):484–92.
16. Bessard A, et al. High antitumor activity of RLI, an interleukin-15 (IL-15)-IL-15 receptor alpha fusion protein, in metastatic melanoma and colorectal cancer. Mol Cancer Ther. 2009;8(9):2736–45.
17. Huang X, et al. Construction and optimization of herpes simplex virus vectors for central nervous system gene delivery based on CRISPR/Cas9-mediated genome editing. Curr Gene Ther. 2022;22(1):66–77.
18. Mueller MM, et al. Autocrine growth regulation by granulocyte colony-stimulating factor and granulocyte macrophage colony-stimulating factor in human gliomas with tumor progression. Am J Pathol. 1999;155(5):1557–67.
19. Obermueller E, et al. Cooperative autocrine and paracrine functions of granulocyte colony-stimulating factor and granulocyte-macrophage colony-stimulating factor in the progression of skin carcinoma cells. Cancer Res. 2004;64(21):7801–12.
20. Pei XH, et al. Granulocyte, granulocyte-macrophage, and macrophage colony-stimulating factors can stimulate the invasive capacity of human lung cancer cells. Br J Cancer. 1999;79(1):40–6.
21. Castro F, et al. Interferon-gamma at the crossroads of tumor immune surveillance or evasion. Front Immunol. 2018;9:847.
22. Su X et al. Breast cancer-derived GM-CSF regulates arginase 1 in myeloid cells to promote an immunosuppressive microenvironment. J Clin Invest, 2021. 131(20).
23. Zhang Y, et al. CircASPH enhances Exosomal STING to facilitate M2 macrophage polarization in colorectal cancer. Inflamm Bowel Dis. 2023;29(12):1941–56.
24. Miao L, et al. Targeting the STING pathway in tumor-associated macrophages regulates innate immune sensing of gastric cancer cells. Theranostics. 2020;10(2):498.
25. Jeong J, Suh Y, Jung K. Context drives diversification of monocytes and neutrophils in orchestrating the tumor microenvironment. Front Immunol. 2019;10:1817.
26. Lazarus HM, et al. Recombinant GM-CSF for diseases of GM-CSF insufficiency: correcting dysfunctional mononuclear phagocyte disorders. Front Immunol. 2023;13:1069444.
27. Kusmartsev S, et al. Antigen-specific Inhibition of CD8 + T cell response by immature myeloid cells in cancer is mediated by reactive oxygen species. J Immunol. 2004;172(2):989–99.
28. Zhang H, et al. Myeloid-derived suppressor cells inhibit T cell proliferation in human extranodal NK/T cell lymphoma: a novel prognostic indicator. Cancer Immunol Immunother. 2015;64:1587–99.
29. Lu Z, et al. Epigenetic therapy inhibits metastases by disrupting premetastatic niches. Nature. 2020;579(7798):284–90.
30. Esquerré M, et al. Human regulatory T cells inhibit polarization of T helper cells toward antigen-presenting cells via a TGF-β-dependent mechanism. Proc Natl Acad Sci. 2008;105(7):2550–5.
31. Bauzon M, Hermiston T. Armed therapeutic viruses - a disruptive therapy on the horizon of cancer immunotherapy. Front Immunol. 2014;5:74.
32. Conry RM, et al. Talimogene Laherparepvec: first in class oncolytic virotherapy. Hum Vaccin Immunother. 2018;14(4):839–46.
33. Breitbach CJ, et al. Pexa-Vec double agent engineered vaccinia: oncolytic and active immunotherapeutic. Curr Opin Virol. 2015;13:49–54.
34. Kaufman HL, et al. Local and distant immunity induced by intralesional vaccination with an oncolytic herpes virus encoding GM-CSF in patients with stage IIIc and IV melanoma. Ann Surg Oncol. 2010;17(3):718–30.
35. Mueller MM, Fusenig NE. Constitutive expression of G-CSF and GM-CSF in human skin carcinoma cells with functional consequence for tumor progression. Int J Cancer. 1999;83(6):780–9.
36. Braun B, et al. Expression of G-CSF and GM-CSF in human meningiomas correlates with increased tumor proliferation and vascularization. J Neurooncol. 2004;68(2):131–40.
37. Ninck S, et al. Expression profiles of angiogenic growth factors in squamous cell carcinomas of the head and neck. Int J Cancer. 2003;106(1):34–44.
38. Huang D, et al. Epstein-Barr Virus-Induced VEGF and GM-CSF drive nasopharyngeal carcinoma metastasis via recruitment and activation of macrophages. Cancer Res. 2017;77(13):3591–604.
39. Morales JK, et al. GM-CSF is one of the main breast tumor-derived soluble factors involved in the differentiation of CD11b-Gr1-bone marrow progenitor cells into myeloid-derived suppressor cells. Breast Cancer Res Treat. 2010;123:39–49.
40. Thorn M, et al. Tumor-associated GM-CSF overexpression induces Immunoinhibitory molecules via STAT3 in myeloid-suppressor cells infiltrating liver metastases. Cancer Gene Ther. 2016;23(6):188–98.
41. Bourgeois-Daigneault MC, et al. Oncolytic vesicular stomatitis virus expressing interferon-γ has enhanced therapeutic activity. Mol Ther Oncolytics. 2016;3:16001.
42. Su C, et al. Immune gene-viral therapy with triplex efficacy mediated by oncolytic adenovirus carrying an interferon-gamma gene yields efficient antitumor activity in immunodeficient and immunocompetent mice. Mol Ther. 2006;13(5):918–27.
43. Cook J, et al. Clinical activity of single-dose systemic oncolytic VSV virotherapy in patients with relapsed refractory T-cell lymphoma. Blood Adv. 2022;6(11):3268–79.
44. Berner V, et al. IFN-gamma mediates CD4 + T-cell loss and impairs secondary antitumor responses after successful initial immunotherapy. Nat Med. 2007;13(3):354–60.
45. Castillo EF, Schluns KS. Regulating the immune system via IL-15 transpresentation. Cytokine. 2012;59(3):479–90.
46. Lodolce JP, et al. Regulation of lymphoid homeostasis by interleukin-15. Cytokine Growth Factor Rev. 2002;13(6):429–39.
47. Guo Y, et al. Immunobiology of the IL-15/IL-15Rα complex as an antitumor and antiviral agent. Cytokine Growth Factor Rev. 2017;38:10–21.
48. Mueller YM, et al. IL-15 enhances survival and function of HIV-specific CD8 + T cells. Blood. 2003;101(3):1024–9.
49. Ghouse SM, et al. Oncolytic herpes simplex virus encoding IL12 controls triple-negative breast cancer growth and metastasis. Front Oncol. 2020;10:384.
50. Ramelyte E, et al. Oncolytic virotherapy-mediated anti-tumor response: a single-cell perspective. Cancer Cell. 2021;39(3):394–406. e4.
51. Ma W, He H, Wang H. Oncolytic herpes simplex virus and immunotherapy. BMC Immunol. 2018;19:1–11.
52. Feola S, et al. Oncolytic immunovirotherapy: A long history of crosstalk between viruses and immune system for cancer treatment. Volume 236. Pharmacology & therapeutics; 2022. p. 108103.
53. Xia M, et al. Graphene oxide arms oncolytic measles virus for improved effectiveness of cancer therapy. J Exp Clin Cancer Res. 2019;38(1):408.
54. Wang Y, et al. Liposome encapsulation of oncolytic virus M1 to reduce immunogenicity and immune clearance in vivo. Mol Pharm. 2019;16(2):779–85.
55. Aoyama K, et al. Liposome-encapsulated plasmid DNA of telomerase-specific oncolytic adenovirus with stealth effect on the immune system. Sci Rep. 2017;7(1):14177.
56. Lv P, et al. Genetically engineered cell membrane nanovesicles for oncolytic adenovirus delivery: A versatile platform for Cancer virotherapy. Nano Lett. 2019;19(5):2993–3001.
57. Nosaki K, et al. A novel, polymer-coated oncolytic measles virus overcomes immune suppression and induces robust antitumor activity. Mol Ther Oncolytics. 2016;3:16022.
58. Du W, et al. Stem cell-released oncolytic herpes simplex virus has therapeutic efficacy in brain metastatic melanomas. Proc Natl Acad Sci U S A. 2017;114(30):E6157–65.
59. Draganov DD, et al. Delivery of oncolytic vaccinia virus by matched allogeneic stem cells overcomes critical innate and adaptive immune barriers. J Transl Med. 2019;17(1):100.

Publisher's note